Poster Reprint

ASMS 2023
Poster number MP 398

A hybrid simulation-experimental approach for the design of a mass spectrometer pumping system

Tong Chen, Mark Werlich, John Nguyen

Agilent Technologies, Santa Clara, CA

Introduction

The pumping system of a mass spectrometer is critical for achieving the performance requirements, e.g., resolution, sensitivity, etc. In specific, a Q-TOF mass spectrometer typically includes a lens system in front of the TOF mass analyzer to collimate the ion beam exiting from the preceding ion guide which is usually a collision cell. The lens system requires a high vacuum to minimize the stochastic ion-neutral scattering and consequently improve the collimation of the ion beam. However, the preceding collision cell is usually operated at a pressure which is several orders of magnitude higher than the desired pressure for the lens system. Therefore, a careful design of the pumping system and the manifold with appropriate conductance is required to accommodate the gas load to the lens system imposed by the collision cell. We herein present a hybrid approach involving theoretical analysis, simulation, and experimental validation for the design of a pumping system to accommodate a novel collision cell [1] integrated to the Revident LC/Q-TOF.

Theoretical Analysis

TOF mass analyzer distinguishes ions by measuring the flight time of ions from the pusher to the detector. The flight time for ions of the same *m/z* follows a bell-shaped distribution. In one definition, the resolution is inversely proportional to the standard deviation of the flight time σ_T. Excluding the mechanical and electrical imperfections, the variance of the flight time σ_T^2 is calculated as

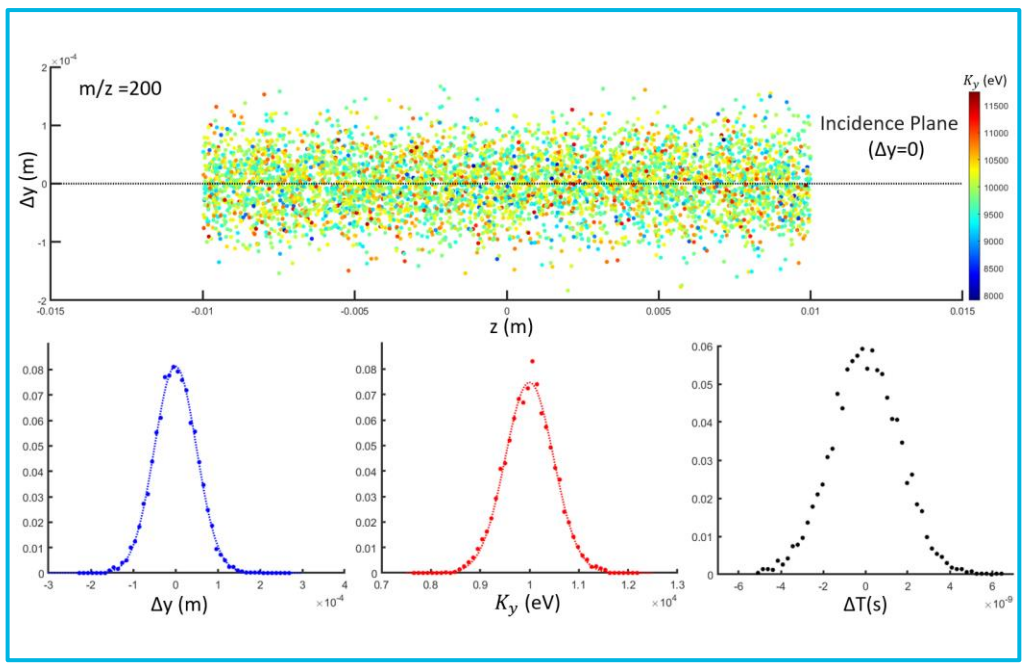

Figure 1. Simulation: an ensemble of 5E3 ions of 200 Da (z=1) arriving at the incidence plane of the detector with the incremental displacement Δy and the incident kinetic energy Ky following normal distributions, and the distribution of the incremental flight time ΔT.

Theoretical Analysis

$$\sigma_T{}^2 = E\left[\frac{(\Delta y)^2}{K_y}\right]\cdot\frac{m}{2} = \sigma_y{}^2\cdot E[\frac{1}{K_y}]\cdot\frac{m}{2}$$

Its derivative with respect to mass is denoted as

$$S \equiv \frac{\partial\sigma_T{}^2}{\partial m} = \frac{1}{2}\sigma_y{}^2\cdot E[\frac{1}{K_y}] \qquad (\text{Note: } E[\tfrac{1}{K_y}] \neq \tfrac{1}{E[K_y]})$$

which represents the slope of the fitting line in the plot of the flight time variance σ_T^2 vs. mass shown in Fig 2.

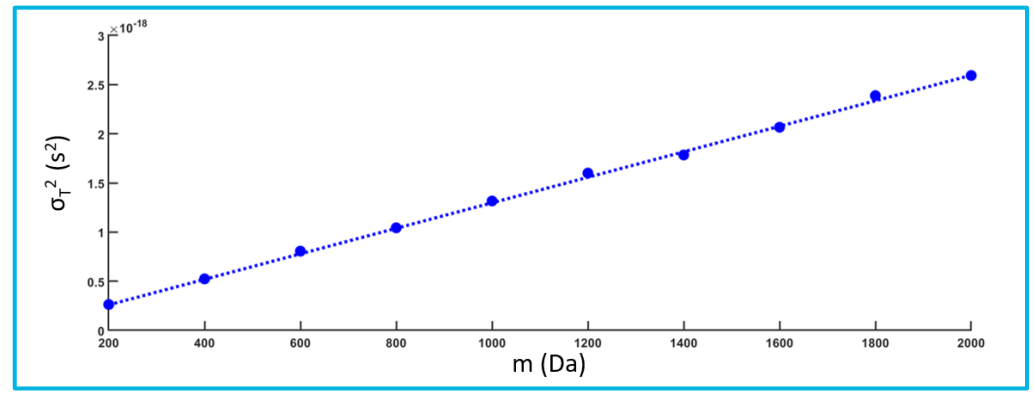

Figure 2. σ_T^2 versus m based on the simulation outcomes of 10 ensembles of singly charged ions with varying masses, subjected to a linear fit.

It is noted that E[1/Ky] ≠ 1/E[Ky]=1/μ_{Ky}, and E[1/Ky] does not even exist if Ky follows a normal distribution. However, the range of Ky is finite in practice. Thus, E[1/Ky] can be approximated by the definite integral over a truncated normal distribution as follow

$$E^*[\frac{1}{K_y}] = \int_{\mu-\alpha\sigma}^{\mu+\alpha\sigma}\frac{1}{K_y}\cdot f(K_y)dK_y$$

$$= \frac{1}{\mu_{K_y}}\cdot\left\{\text{erf}(\alpha/\sqrt{2}) + \frac{\sigma_{K_y}{}^2}{\mu_{K_y}{}^2}\left[\text{erf}(\alpha/\sqrt{2}) - \sqrt{2/\pi}\alpha e^{-\alpha^2/2}\right]\right\}$$

Note, the second term in the curly bracket denoted as $C(\alpha)$ approaches 1 when $\sigma_{Ky} << \mu_{Ky}$ and $\alpha \geq 3$, shown in Fig 3, which are valid conditions in practice.

The analysis above suggests that the coefficient S only depends on the spatial variance σ_y, and the kinetic energy's mean μ_{Ky} and variance σ_{Ky}, which are determined by the optics of the mass analyzer and the initial conditions of the ion beam, independent of the mechanical and electrical imperfections.

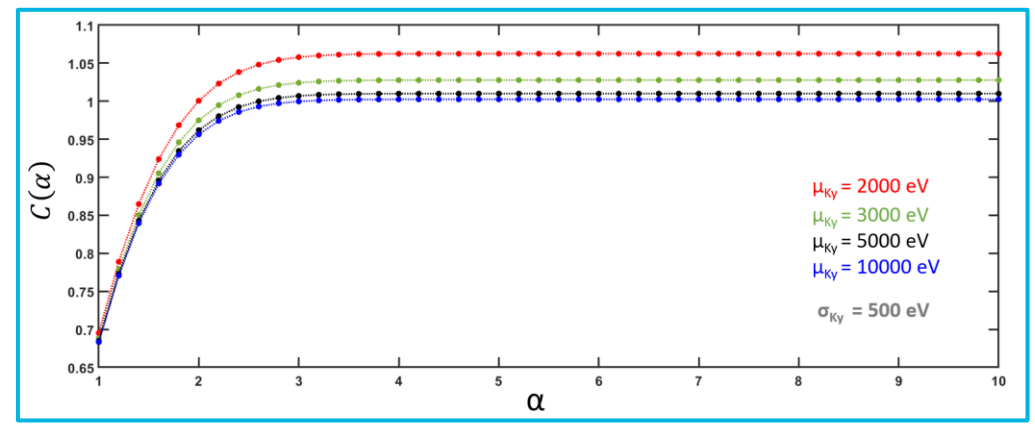

Figure 3. Compensation factor C(α) versus α.

Simulation and Experiments

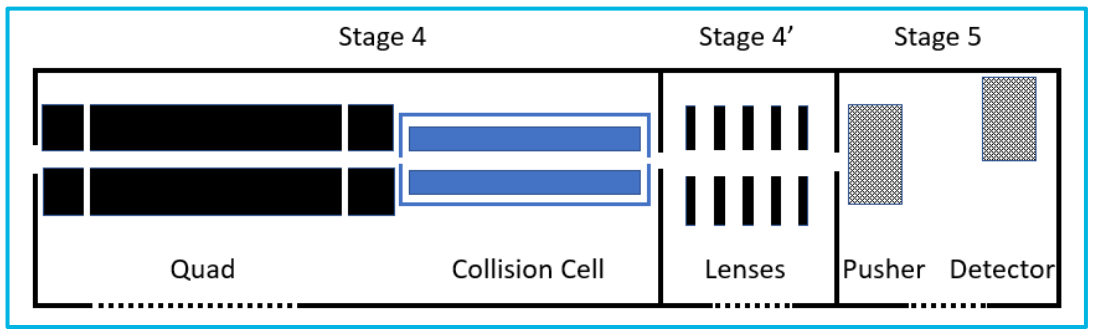

Figure 4. Scheme of a portion of a Q-TOF instrument.

To characterize the impacts of the pressure to the resolution, we performed experiments on an Agilent 6546 LC/Q-TOF instrument (Fig. 4) with calibrant samples of various masses (singly charged ions). In the experiments, the pressure of the lens system was varied by adjusting the rotation speed of the turbopump of the corresponding vacuum stage and the conductance to the adjacent stages. Fig. 5 shows that the flight time variance σ_T^2 increases with the pressure for all masses. However, the rate of increase is mass dependent, i.e., the increase of σ_T^2 for heavier ions is faster than lighter ions, exhibiting nonlinearity in the plot of σ_T^2 vs. mass.

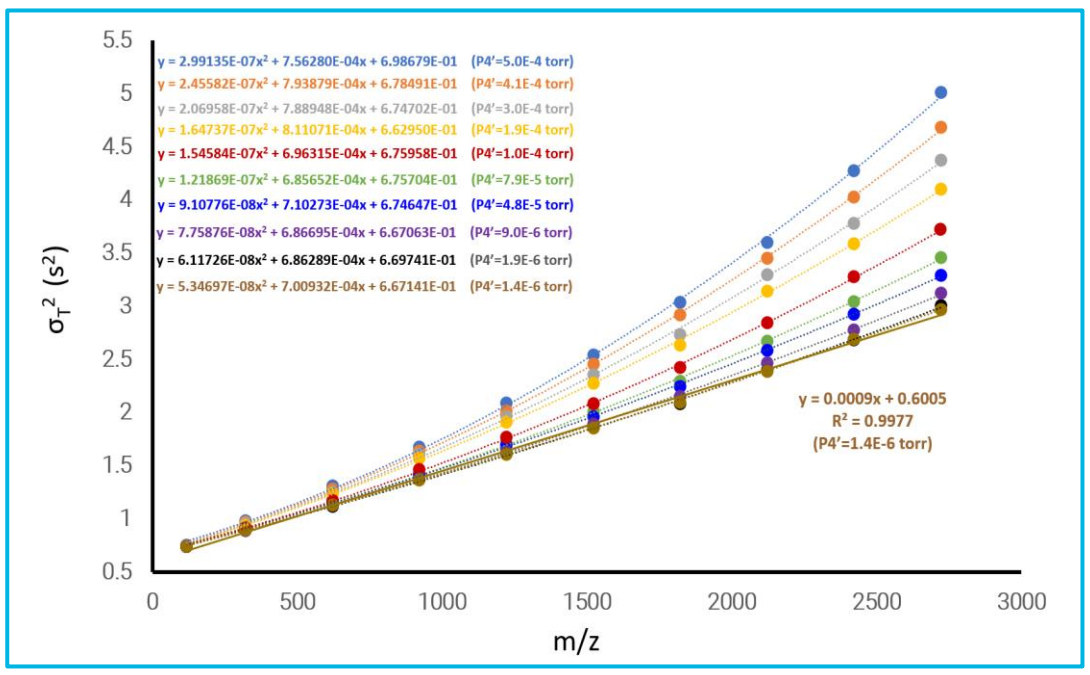

Figure 5. σ_T^2 versus mass for different pressures of the lens system. All the ions are singly charged.

The nonlinearity can be understood as follow. The ion-neutral collisions in the lens system would increase the divergence of the ion beam entering the pusher which is the first optical element of the TOF mass analyzer. As a result, the spatial variance σ_y increases, leading to an increase in the coefficient S. The increase of σ_y is mass dependent, because heavier ions typically have larger cross-sectional areas, resulting in more collisions with neutrals and thus greater increases in the ion beam divergence at the initial state. Therefore, the coefficient S increases with the mass, reflected by the nonlinearity in the relation between the flight time variance and the mass. The nonlinearity can serve as a measure of the sufficiency of vacuum, which would be diminished in the condition of enough vacuum.

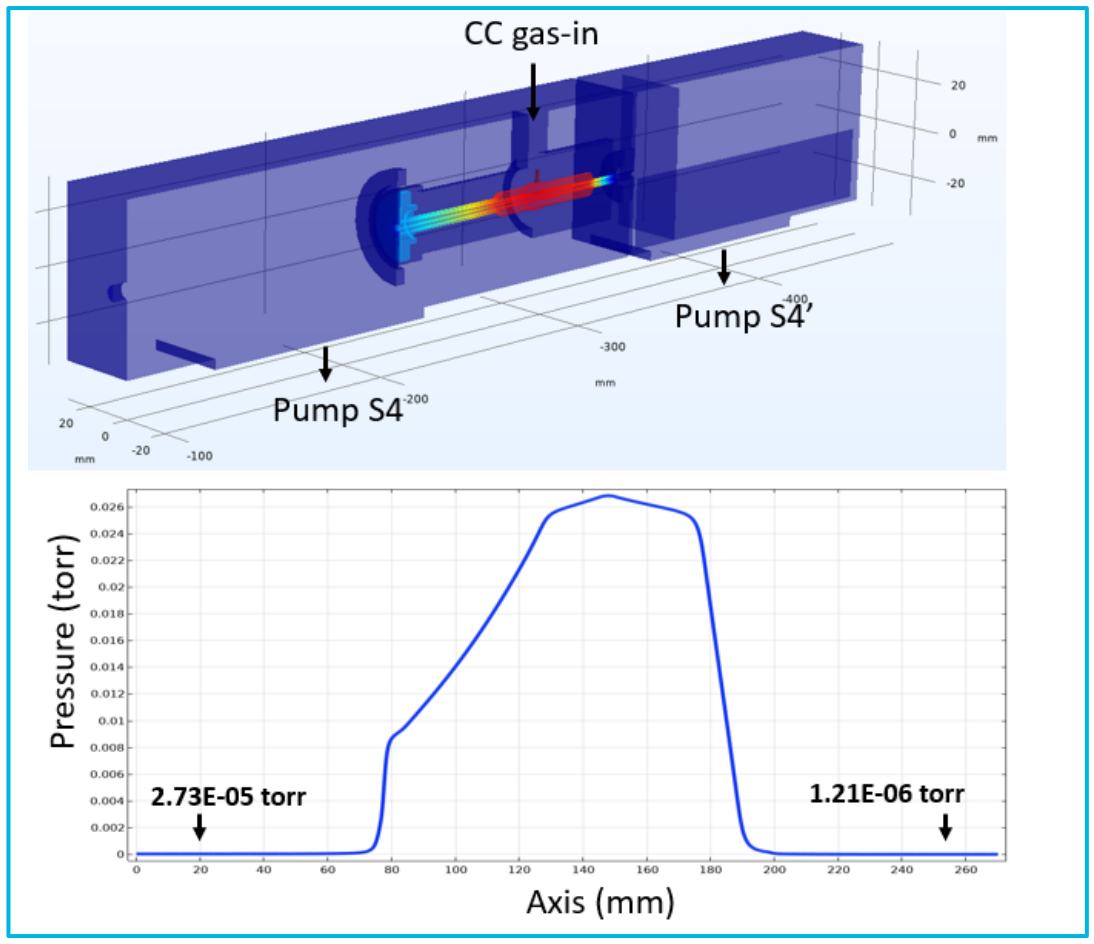

Figure 6. Simulation: pressure profiles of collision cell and adjacent stages based on the optimized pumping speeds.

Based on the results shown in Fig.5 and the requirements in resolution for the next-gen instrument, it is determined that the pressure of the lens system should be lower than 1.5E-6 torr. Also, the new collision cell requires an appropriate internal pressure profile (Fig. 6) to efficiently perform designated functions, e.g., CID fragmentation. With these restrictions, simulation is performed in COMSOL [2] to calculate the required pumping speed for the vacuum stage of the lens system, yielding a value of ~100 l/s. The simulation is followed by the experimental verification, in which the conductance of the pumping port is adjusted by a cover plate of tailored size to yield an effective pumping speed equal to the target value (Fig. 7).

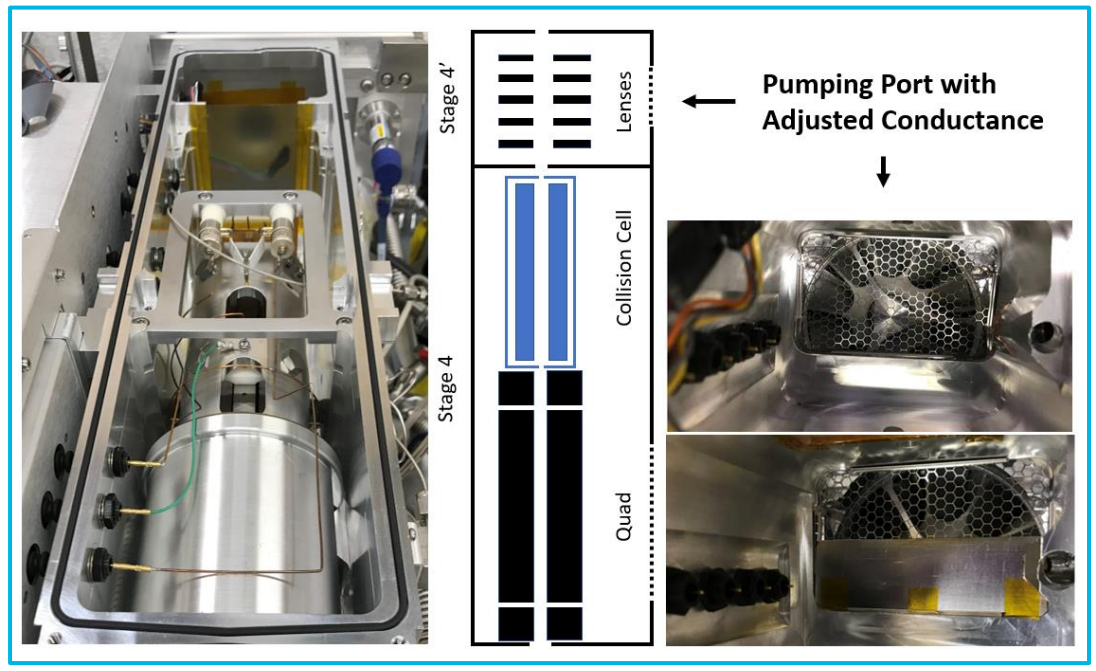

Figure 7. Adjusted conductance of pumping port at the stage of the lens system (Stage 4') by a tailored plate.

Results and Discussion

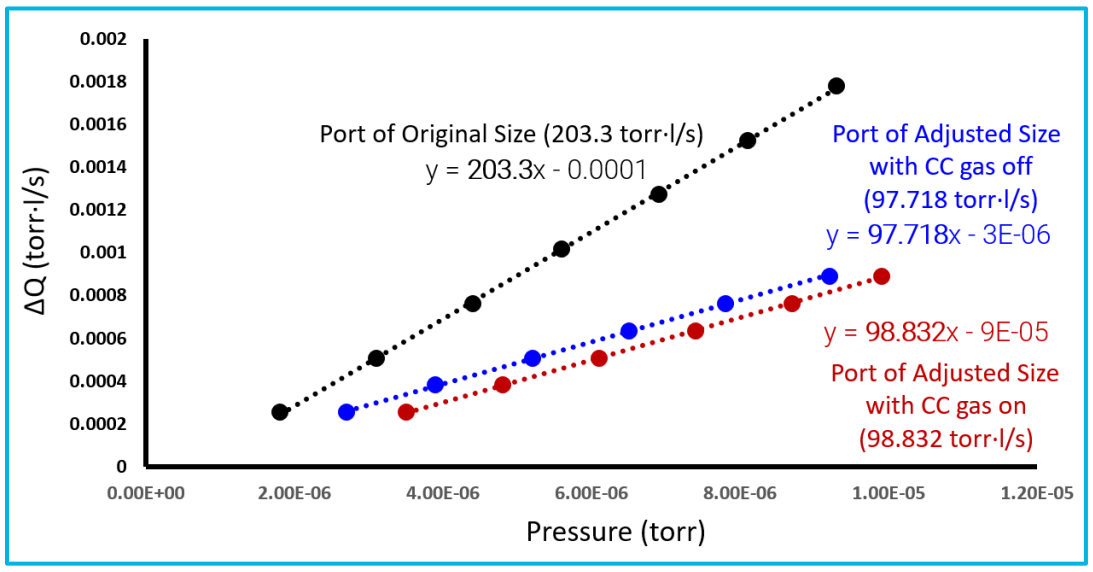

Figure 8. Measured throughputs versus pressures of the lens system (Stage 4') under various conditions.

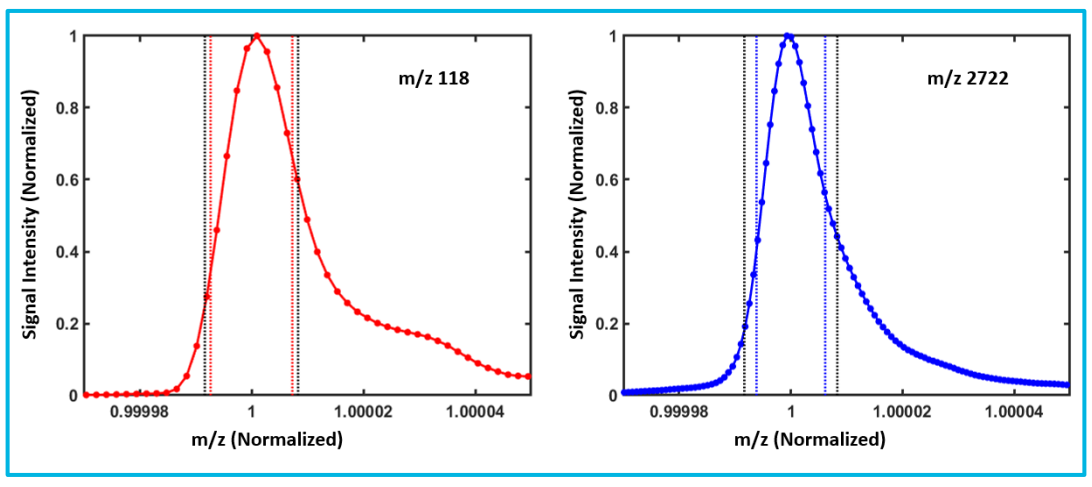

Figure 9. Peak profiles for *m/z* 118 and 2722 collected in the experiments with the adjusted pumping speed.

The effective pumping speed of the lens system (Stage 4') is derived by calculating the slope of the linear fitting line in the plot of measured throughputs versus pressures (Fig. 8). With the adjusted pumping speed, MS experiments are conducted to verify that the required resolution across the required range of *m/z* is achieved (Fig. 9). The intervals marked by the black dash lines correspond to the peak width of the required resolution, whereas the intervals marked by the red and blue dash lines correspond to the peak widths of the measured resolutions for *m/z* 118 and *m/z* 2722 respectively.

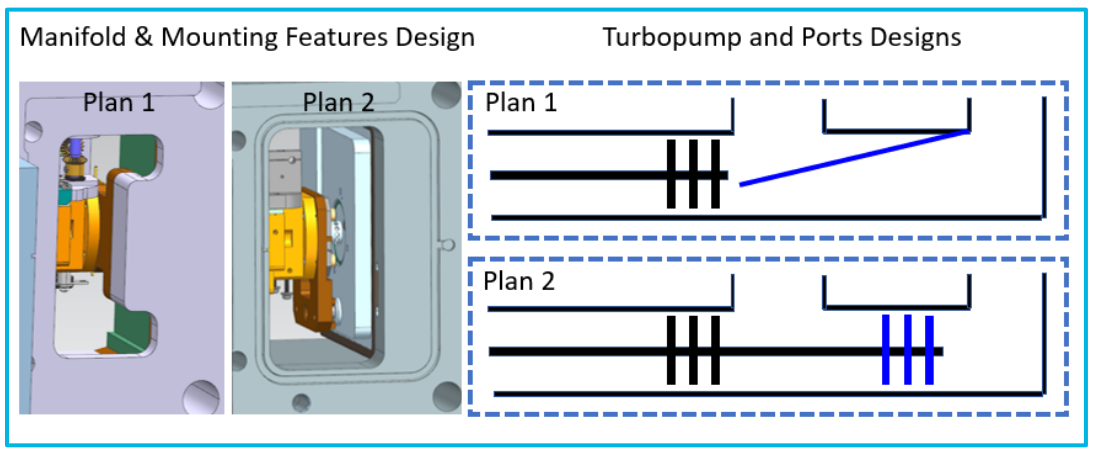

Figure 10. A) Designs of the manifold with lens mounts to produce the required conductance. B) Designs of the turbopump to produce required pumping speeds.

Following the determination of the pumping speed of the lens system, the manifold with the lens mounts and the modified turbopump with an additional port are designed for producing appropriate conductance and pumping speed respectively which are combined to achieve the predetermined effective pumping speed of the lens system. Two schemes are explored and compared (Fig. 10). Plan 2 is selected to deliver the final solution of the pumping system shown in Fig. 11.

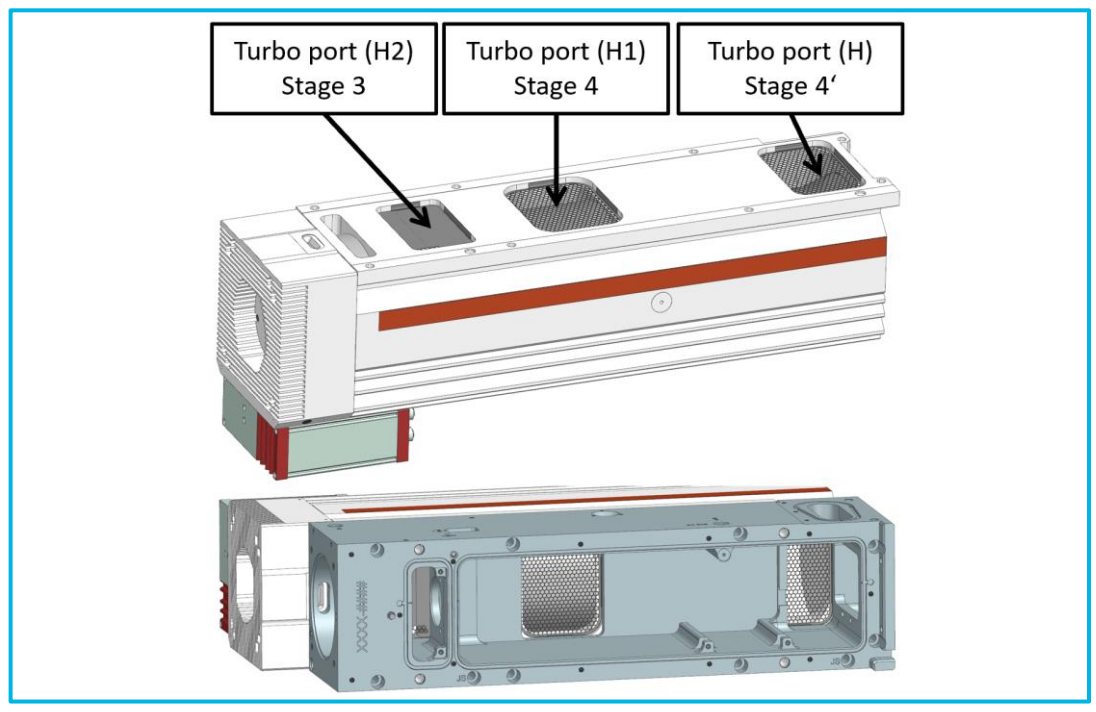

Figure 11. CAD modes of the new pumping system.

Conclusions

A new pumping system is designed to accommodate the integration of a novel collision cell into the Revident LC/Q-TOF. A systematic approach is employed for the design of the pumping system, including theoretical analysis, simulation, and experimental testing and validation.

- A characteristic coefficient is derived to serve as a measure of the sufficiency of vacuum.
- Critical parameters, e.g., the required pumping speed, are calculated in simulation, followed by experimental testing and verification.
- The approach is applicable to the design of pumping systems for other types of mass spectrometers.

References

[1] Pollum, L.L., Wang, H., Newton, K.R., Tichy, S.E.. ASMS Annual Conference 2018.

[2] COMSOL Multiphysics® v. 5.6. COMSOL AB, Stockholm, Sweden.

https://www.agilent.com/en/promotions/asms

DE02567104

Published in USA, May 31,2023

Agilent
Trusted Answers